

Vibrations of Molecules and Solids

Charbel Tannous

▶ **To cite this version:**

Charbel Tannous. Vibrations of Molecules and Solids. Master. France. 2018. hal-03779719

HAL Id: hal-03779719
https://hal.science/hal-03779719

Submitted on 17 Sep 2022

HAL is a multi-disciplinary open access archive for the deposit and dissemination of scientific research documents, whether they are published or not. The documents may come from teaching and research institutions in France or abroad, or from public or private research centers.

L'archive ouverte pluridisciplinaire **HAL**, est destinée au dépôt et à la diffusion de documents scientifiques de niveau recherche, publiés ou non, émanant des établissements d'enseignement et de recherche français ou étrangers, des laboratoires publics ou privés.

Vibrations of Molecules and Solids

C. Tannous
Université de Brest, Lab-STICC, CNRS-UMR 6285, F-29200 Brest, FRANCE
(Dated: September 17, 2022)

Vibrations in molecules and in condensed matter are described and discussed. Forces between neighboring atoms are considered classically as radial or angular meaning that vibrational potential energy is due either to length change in bonding distance (two-body effect) or angle change (bending) of bonding configuration (three-body effect). After describing the historical (Diamond case) and later the general theory of vibrations in condensed matter, we apply it to the 1D diatomic chain to explain the notions of acoustic and optic phonons from their dispersion and density of states points of view. Application to Graphene is later described as a general methodology for phonon dispersion and density of states determination.

PACS numbers: 61.48.De, 63.22.m, 63.20.Dj, 81.05.Uw, 71.15.Mb

Contents

I. Introduction 1

II. Molecular vibrations: Triangular molecule 2

III. Crystal vibrations: Early approaches and the Entropy catastrophe 3

IV. General description of crystal vibrations 5
A. Acoustic and Optic modes 7
B. Vibrational density of states 8

V. Application to Graphene 10

A. Arbitrary 3D spring deformation energies 13
1. Stretching deformation energy 14
2. Bending deformation energy 15

B. Note on the Bulk modulus 15

References 16

I. INTRODUCTION

Vibrations in molecules and solids are discussed using mass and spring description of deformation energy then applied to the case of a triangular molecule in order to review thoroughly the handling of vibration coordinates while accounting for symmetry constraints allowing writing the equations of motion and determination of eigenmodes.

The example of a triangular molecule is not trivial and displays symmetries that belong to hexagonal systems like graphite and graphene and should be handled with care in order to get the eigenmodes properly.

Historically Diamond was used as an example of a vibrating structure to explain its specific heat leading Einstein and later Debye to study it in a pioneering way that opened fully the modern field of condensed matter vibrations along with its thermodynamics and its relations to other physical properties (optical, mechanical, thermal...).

Afterwards we describe the general theory of vibrations in condensed matter and apply it to the case of 1D diatomic chain to illustrate acoustic and optic phonons and move later to the description of Graphene.

The vibration formalism when devoted to Graphene relies on several possible oscillation scenarios that are tested experimentally with the measurement of many structural, mechanical and thermodynamic quantities that are discussed accordingly.

II. MOLECULAR VIBRATIONS: TRIANGULAR MOLECULE

While the example of a triangular molecule is very pedagogic, yet it bears some of the symmetries that we encounter in the solid state with graphite and graphene structures whose vibrations are analyzed in section V.

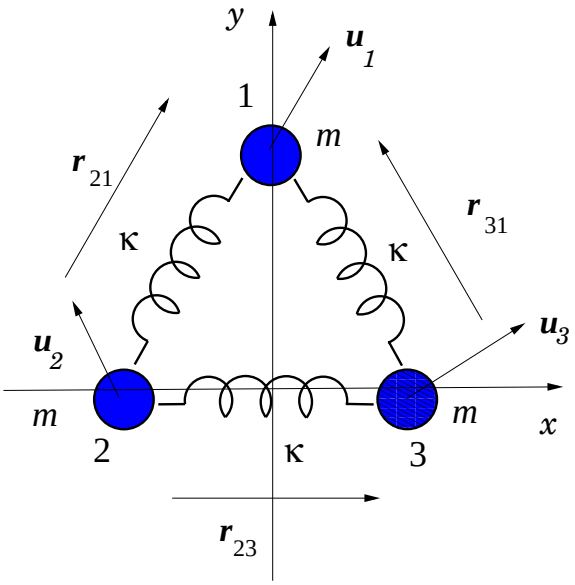


Fig. 1: (Color on-line) Triangular molecule[1,2] made of atoms with same m, the atomic mass and κ the spring constant corresponding to binding energy between atomic neighbors. Vectors linking neighboring atoms are: $\boldsymbol{r_{23}}, \boldsymbol{r_{31}}$ and $\boldsymbol{r_{21}}$, whereas small displacements of the atomic masses m are given by: $\boldsymbol{u}_i = (x_i, y_i), i = 1, 2, 3$.

Following the labeling of Fig. 1 we have the unit vectors linking neighboring atoms $\widehat{\boldsymbol{r_{23}}} = (1, 0)$, $\widehat{\boldsymbol{r_{31}}} = (-\frac{1}{2}, \frac{\sqrt{3}}{2})$ and $\widehat{\boldsymbol{r_{21}}} = (\frac{1}{2}, \frac{\sqrt{3}}{2})$.

The displacements of the masses[1–3] are: $\boldsymbol{u}_i = (x_i, y_i), i = 1, 2, 3$. Applying formula A3 we get the potential energy:

$$V = \frac{1}{2}\kappa\left[\frac{1}{2}(x_2 - x_1) + \frac{\sqrt{3}}{2}(y_2 - y_1)\right]^2 + \frac{1}{2}\kappa\left[-\frac{1}{2}(x_1 - x_3) + \frac{\sqrt{3}}{2}(y_1 - y_3)\right]^2 + \frac{1}{2}\kappa\left[\frac{1}{2}(x_2 - x_3)\right]^2 \tag{1}$$

The kinetic energy writes:

$$T = \frac{1}{2}m\left[\dot{x}_1^2 + \dot{y}_1^2 + \dot{x}_2^2 + \dot{y}_2^2 + \dot{x}_3^2 + \dot{y}_3^2\right] \tag{2}$$

In order to find the modes it suffices to write down the Lagrangian and derive Euler-Lagrange equations of motion.

$$\frac{d}{dt}\left(\frac{\partial T}{\partial \dot{q}_i}\right) + \frac{\partial V}{\partial q_i} = 0, \quad q_i = x_i,\ i = 1, 2, 3, \quad q_i = y_i,\ i = 4, 5, 6 \tag{3}$$

We substitute $q_i = a_i \exp(j\omega t)$ with $\omega = \sqrt{\frac{\lambda\kappa}{m}}$ obtaining from the Lagrange equations 3 the secular equation:

$$D(\lambda) = \begin{vmatrix} \frac{1}{2} - \lambda & 0 & -\frac{1}{4} & -\frac{1}{4}\sqrt{3} & -\frac{1}{4} & \frac{1}{4}\sqrt{3} \\ 0 & \frac{3}{2} - \lambda & -\frac{1}{4}\sqrt{3} & -\frac{3}{4} & \frac{1}{4}\sqrt{3} & -\frac{3}{4} \\ -\frac{1}{4} & -\frac{1}{4}\sqrt{3} & \frac{5}{4} - \lambda & \frac{1}{4}\sqrt{3} & -1 & 0 \\ -\frac{1}{4}\sqrt{3} & -\frac{3}{4} & \frac{1}{4}\sqrt{3} & \frac{3}{4} - \lambda & 0 & 0 \\ -\frac{1}{4} & \frac{1}{4}\sqrt{3} & -1 & 0 & \frac{3}{4} - \lambda & -\frac{1}{4}\sqrt{3} \\ \frac{1}{4}\sqrt{3} & -\frac{3}{4} & 0 & 0 & -\frac{1}{4}\sqrt{3} & \frac{3}{4} - \lambda \end{vmatrix} = 0 \tag{4}$$

Expanding the determinant, we get: $D(\lambda) = \lambda^6 - 6\lambda^5 + 45\lambda^4/4 - 27\lambda^3/4$ and the eigenvalues are $\lambda = 0$, $\lambda = 3/2$ and $\lambda = 3$.

The confirmation of these values as well as their multiplicities is given by the plot of $D(\lambda)$ versus λ depicted in fig. 2 and displaying three roots: triple $\lambda = 0$, double $\lambda = 3/2$ and simple $\lambda = 3$ implying that $D(\lambda)$ can be factored as $D(\lambda) = \lambda^3(\lambda - 3/2)^2(\lambda - 3)$.

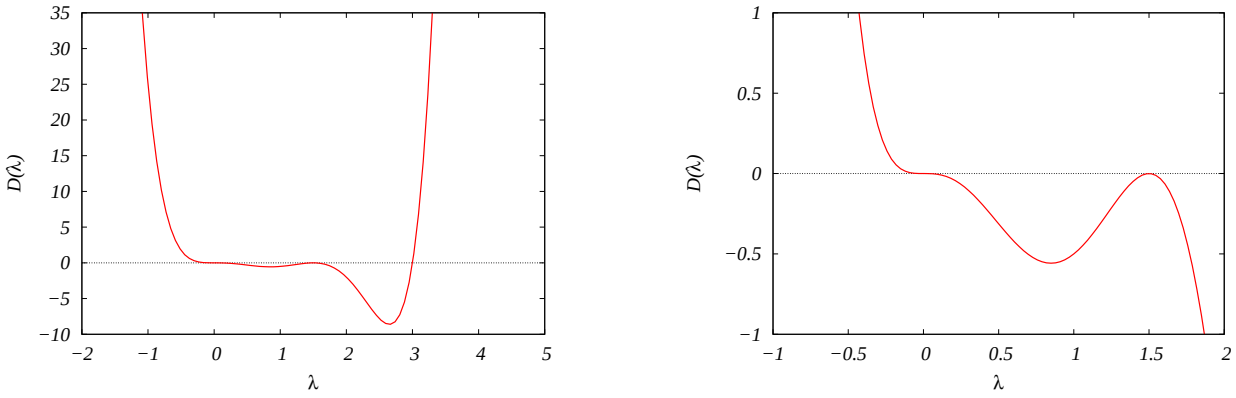


Fig. 2: (Color on-line) From the local aspect (cubic, parabolic or linear) of the secular determinant $D(\lambda)$ around the crossings with the λ axis as depicted in the right figure, we infer that we have three solutions: triple $\lambda = 0$, double $\lambda = 3/2$ and simple $\lambda = 3$

III. CRYSTAL VIBRATIONS: EARLY APPROACHES AND THE ENTROPY CATASTROPHE

In the classical mass-spring model picture of a 3D solid, a mole is made of $3N_A$ vibrating atoms/molecules where N_A is Avogadro number.

Thus the number of degrees of freedom required by the equipartition theorem is $6N_A$ since each vibrating atom/molecule is made of a mass m with kinetic energy $\frac{m\dot{x}^2}{2}$ and a spring with constant κ yielding potential energy $\frac{\kappa x^2}{2}$ where $x, \dot{x}$ are coordinate and velocity along some direction. Thus the total energy is $U = 6N_A \times \frac{k_B T}{2} = 3N_A k_B T$ yielding a constant volume specific heat given by: $C_V = \left(\frac{\partial U}{\partial T}\right)_V = 3N_A k_B$. This is the Dulong-Petit law stating that C_V saturates at all temperatures.

However, the constant volume specific heat is given by: $C_V = T\left(\frac{\partial S}{\partial T}\right)_V$ implying that $\frac{C_V}{T} = \left(\frac{\partial S}{\partial T}\right)_V$ and since C_V is constant this may be integrated as: $S = C_V \ln T + C_1$ where C_1 is a constant.

Consequently when $T \to 0K$ $S \to -\infty$. This is the entropy catastrophe (since S should be positive) akin to the ultra-violet catastrophe of the blackbody radiation that was solved by Planck with the introduction of Quantum Mechanics.

In the year 1907, Einstein who was at the time at the Swiss Patent Office and had read 1901 Planck paper, decided to quantize the classical Dulong-Petit law as he quantized the photoelectric effect in 1905.

Following Planck, Einstein considered $3N_A$ quantum oscillators all having the same energy $\hbar\omega_E$ with mean number given by Planck factor $\langle n \rangle = \frac{1}{[\exp(\hbar\omega_E/k_B T)-1]}$, thus the energy becomes $U = 3N_A \hbar\omega_E \langle n \rangle = \frac{3N_A \hbar\omega_E}{[\exp(\hbar\omega_E/k_B T)-1]}$.

Calculating the specific heat, he obtained:

$$C_V = \left(\frac{\partial U}{\partial T}\right)_V = 3N_A k_B \left(\frac{\hbar\omega_E}{k_B T}\right)^2 \frac{\exp(\hbar\omega_E/k_B T)}{[\exp(\hbar\omega_E/k_B T) - 1]^2} \tag{5}$$

Thus we get the two limits: $k_B T \gg \hbar\omega_E, \quad C_V \to 3N_A k_B$ recovering Dulong-Petit in the classical case and when: $k_B T \ll \hbar\omega_E, \quad C_V \to 3N_A k_B \left(\frac{\hbar\omega_E}{k_B T}\right)^2 \exp -(\hbar\omega_E/k_B T)$.

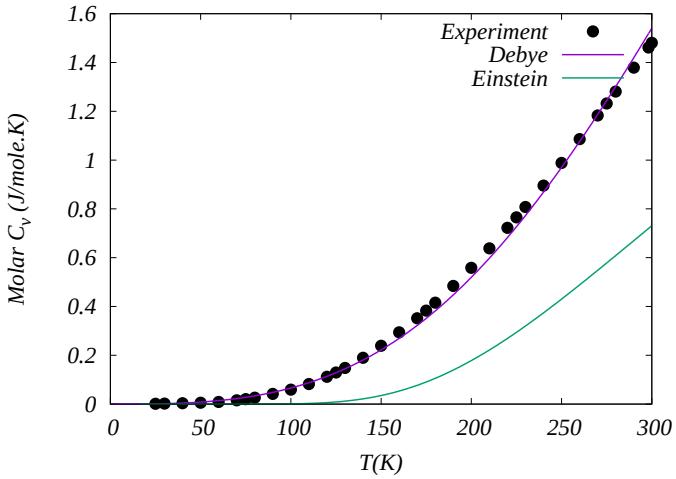


Fig. 3: (Color on-line) Comparison of Debye, Einstein and experimental results of molar C_V for Diamond. Molar C_V is defined in the Debe case as $3f_D(x_D)$, whereas in the Einstein case as $3\left(\frac{\hbar\omega_E}{k_BT}\right)^2 \frac{\exp(\hbar\omega_E/k_BT)}{[\exp(\hbar\omega_E/k_BT)-1]^2}$ and the Debye temperature $\Theta_D = \hbar\omega_D/k_B$ used is 2200K (Pure Diamond Debye temperature is 1860K) whereas the Einstein temperature $\Theta_E = \hbar\omega_E/k_B$ is 1320K. The experimental points are taken from DeSorbo paper[4].

In spite of the fact, Einstein could not know about phonons nor their statistics, he treated them like blackbody photons, obtaining a result showing that the entropy is positive and goes to zero when $T \to 0K$ as required by Nernst third principle of thermodynamics. In order to fit the available results at low temperature of the specific heat of Diamond he used an oscillator energy $\hbar\omega_E$ equivalent to a temperature $\Theta_E = \hbar\omega_E/k_B$ of 1320K (see Kittel[5]).

When new experimental results were obtained on Diamond at low temperature with greater precision, the specific heat appeared to follow Debye T^3 acoustic phonon result and Einstein result was interpreted as valid rather for optic phonons[5]. Very generally, when excitations have an energy gap $\hbar\omega_0$ the specific heat behaves as $\exp -(\hbar\omega_0/k_BT)$.

In the Debye approach, one considers in a 3D crystal a linear dispersion of phonons (see next section) yielding a density of states given by $g_D(\omega) = \frac{V_c\omega^2}{2\pi^2 v_\lambda^3}$ where λ is the acoustic phonon branch with the sound velocity given by v_λ, V_c is the crystal volume and the total vibrational energy for the branch is given by:

$$U_\lambda = \int_0^{\omega_D} d\omega \left(\frac{V_c\omega^2}{2\pi^2 v_\lambda^3}\right) \frac{\hbar\omega}{(\exp(\hbar\omega/k_BT)-1)} \tag{6}$$

This can be rewritten as: $U_\lambda = AT^4 f(x_D)$ with $A = \frac{V_c k_B^4}{2\pi^2 v_\lambda^3 \hbar^3}$ and $f(x_D) = \int_0^{x_D} dx \frac{x^3}{(e^x-1)}$ with $x_D = \frac{\hbar\omega_D}{k_BT} = \frac{\Theta_D}{T}$ where Θ_D is Debye temperature.

The calculation of the specific heat given by $C_V = \left(\frac{\partial U}{\partial T}\right)_V = 4AT^3 f(x_D) + AT^4 \frac{\partial f(x_D)}{\partial T}$.

The derivation of $f(x_D)$ with respect[6] to T yields $AT^3\left(\frac{-\hbar\omega_D}{k_BT^2}\right)\frac{x_D^3}{(e^{x_D}-1)}$. Thus we have:

$$C_V = 4AT^3 \int_0^{x_D} dx \frac{x^3}{(e^x-1)} - AT^4\left(\frac{\hbar\omega_D}{k_BT^2}\right)\frac{x_D^3}{(e^{x_D}-1)} \tag{7}$$

This result was also obtained by Debye[7], nevertheless several authors[8] in the literature give the result:

$$C_V = 3Nk_B f_D(x_D), \qquad f_D(x_D) = \frac{3}{x_D^3}\int_0^{x_D} dt \frac{t^4 e^t}{(e^t-1)^2} \tag{8}$$

Both expressions of C_V are same since $A = \frac{V_c k_B^4}{2\pi^2 v_\lambda^3 \hbar^3}$ and ω_D can be evaluated from the conservation of total modes which is given by: $\int_0^{\omega_D} g_D(\omega)d\omega = 3N$.

This means $\omega_D^3 = \frac{18N\pi^2 v_\lambda^3}{V_c}$ yielding $A\left(\frac{\hbar\omega_D}{k_B T}\right)^3 = 9Nk_B$ implying the equality of both C_V expressions $3Nk_B f_D(x_D)$ and $4AT^3\int_0^{x_D} dx\frac{x^3}{(e^x-1)} - AT^4\left(\frac{\hbar\omega_D}{k_B T^2}\right)\frac{x_D^3}{(e^{x_D}-1)}$.

In the literature, the dilemma is that most authors call both functions appearing in U_λ and C_V as Debye functions whereas in the Mathematics[9] literature, the Debye function is given by $\int_0^x dx\frac{x^3}{(e^x-1)}$.

Note however that recently Dubinov *et al.*[10] gave a classification of both types of Debye functions $D_1(n,x), D_2(n,x)$:

$$D_1(n,x) = \frac{n}{x^{n+1}}\int_0^x dt\frac{t^n}{(e^t-1)}, \qquad D_2(n,x) = \frac{n}{x^n}\int_0^x dt\frac{t^{n+1}e^t}{(e^t-1)^2} \tag{9}$$

Actually, there is no need to define Type 2 Debye functions since an integration by part is sufficient to transform the function $f_D(x) = \frac{3}{x^3}\int_0^x dt\frac{t^4 e^t}{(e^t-1)^2}$ into the regular Type 1 Debye function as defined by Mathematical Tables[9].

In effect, define $u = t^4, du = 4t^3 dt$ and $v = -\frac{1}{(e^t-1)}, dv = \frac{dt}{(e^t-1)^2}$, then one writes:

$$f_D(x) = \frac{3}{x^3}\int_0^x dt\ udv = \frac{3}{x^3}\left([uv]_0^x + \int_0^x dt\frac{4t^3}{(e^t-1)}\right) \tag{10}$$

Thus $f_D(x) = \frac{12}{x^3}\int_0^x dt\frac{t^3}{(e^t-1)} - \frac{3x}{(e^x-1)}$ is defined solely with the type 1 Debye function.

IV. GENERAL DESCRIPTION OF CRYSTAL VIBRATIONS

There are many approaches to describe vibrations in crystals depending on their nature: Metals, Semiconductors (covalent), Ionic (Insulators, Molecular crystals...), Magnetic...

The earliest approach is the mass and spring model, a hybrid approach where the crystal ions are treated classically whereas their vibrations are quantized in order to avoid the entropy catastrophe.

Starting with the mass and spring model, the Hamiltonian of a vibrating crystal is given by[11]

$$\mathcal{H} = \sum_{nli}\frac{M_n}{2}\dot{u}_i^2(n,l) + \frac{1}{2}\sum_{nli}\sum_{ml'j}\Phi_{ij}\begin{pmatrix} m & n \\ l & l'\end{pmatrix}u_i(n,l)u_j(m,l'), \tag{11}$$

where

$$\Phi_{ij}\begin{pmatrix} m & n \\ l & l'\end{pmatrix} = \left[\frac{\partial^2 V}{\partial u_i(n,l)\partial u_j(m,l')}\right]_{eq} \tag{12}$$

V is the ion-ion interaction potential, M_n is the mass of atom n, $u_i(n,l)$ is a small displacement of atom n in the lattice cell l along direction i. $\Phi_{ij}\begin{pmatrix} m & n \\ l & l'\end{pmatrix}$ is the force constant matrix linking an atom n in lattice cell l along direction i to atom m in the lattice cell l' displaced by unit distance along direction j. Symbol eq indicates the second derivative is taken at equilibrium lattice configuration.

The equation of motion of atom n in the lattice cell l is given by:

$$M_n\ddot{u}_i(n,l) = -\sum_{ml'j}\Phi_{ij}\begin{pmatrix} m & n \\ l & l'\end{pmatrix}u_j(m,l'). \tag{13}$$

Exploiting crystal translational symmetry, the small displacement can be written as a plane-wave:

$$u_i(n,l) = \frac{1}{\sqrt{M_n}}u_i^n e^{i(\boldsymbol{k}\cdot\boldsymbol{r}_n(l)-\omega t)}, \tag{14}$$

where u_i^n is the amplitude of vibration of atom n along direction i and $\boldsymbol{r}_n(l)$ is the lattice translation vector.

Using the above expression of $u_i(n,l)$ turns eq. 13 into an eigenvalue equation:

$$\sum_{ml'j} \frac{1}{M_n} \Phi_{ij} \begin{pmatrix} m & n \\ l & l' \end{pmatrix} u_j(m,l') - \omega^2 u_i(n,l) = 0 \tag{15}$$

Thus we define the Fourier transform of the force constant matrix as the dynamical matrix:

$$D_{ij}(mn,\boldsymbol{k}) = \frac{1}{\sqrt{M_m M_n}} \sum_l \Phi_{ij} \begin{pmatrix} m & n \\ l & l' \end{pmatrix} e^{-i\boldsymbol{k}\cdot\boldsymbol{r}_n(l)} \tag{16}$$

This results into the eigenvalue equation:

$$\sum_{m,j} D_{ij}(mn,\boldsymbol{k}) u_j^m = \omega^2 u_i^n \tag{17}$$

The dynamical matrix is Hermitian [$D_{ij} = D_{ji}^*$], thus its eigenvalues are real and yield the vibration spectrum. Eigenvalues are obtained from:

$$|D_{ij}(mn,\boldsymbol{k}) - \omega^2 \delta_{ij}\delta_{mn}| = 0. \tag{18}$$

Force constant matrix $\Phi_{ij} \begin{pmatrix} m & n \\ l & l' \end{pmatrix}$ possess the following properties:

1. $\Phi_{ij} \begin{pmatrix} m & n \\ l & l' \end{pmatrix}$ being a second-order partial differential, thus:

$$\Phi_{ij} \begin{pmatrix} m & n \\ l & l' \end{pmatrix} = \Phi_{ji} \begin{pmatrix} n & m \\ l' & l \end{pmatrix}. \tag{19}$$

2. Translational symmetry implies that $\Phi_{ij} \begin{pmatrix} m & n \\ l & l' \end{pmatrix}$ is a function of $\boldsymbol{r}_m(l)$ - $\boldsymbol{r}_n(l')$. Hence,

$$\Phi_{ij} \begin{pmatrix} m & n \\ l & l' \end{pmatrix} = \Phi_{ij} \begin{pmatrix} m & n \\ 0 & l \end{pmatrix}, \tag{20}$$

   where 0 refers to the origin of coordinates.

3. Invariance of potential energy under rigid body displacement of the whole crystal yields:

$$\sum_{n,l} \Phi_{ij} \begin{pmatrix} m & n \\ 0 & l \end{pmatrix} = 0. \tag{21}$$

4. If the crystal has inversion symmetry then

$$\Phi_{ij} \begin{pmatrix} m & n \\ 0 & l \end{pmatrix} = \Phi_{ij} \begin{pmatrix} m & n \\ 0 & -l \end{pmatrix}. \tag{22}$$

These properties are useful in finding out relations between various force constants. The evaluation of force constants is such that we suppose $\boldsymbol{u}_j(m)$ be the relative displacement of atom m along direction j with respect to atom n. Then the force acting on atom n along direction i due to displacement of atom m only is:

$$f_i = \kappa_m e_i(m) \sum_j \boldsymbol{e}_j(m) \cdot \boldsymbol{u}_j(m), \tag{23}$$

where $\boldsymbol{e(m)}$ is the unit vector along $\boldsymbol{r}_m(l)$ and κ_m the spring constant between n and m atoms. We infer that the total force acting on atom n along direction i due to neighboring atoms is:

$$F_i = \sum_{ml} \kappa_m e_i(m) \sum_j \boldsymbol{e}_j(m) \cdot \boldsymbol{u}_j(m). \tag{24}$$

Comparing the above equation with equation(19) and using the definition of $\Phi_{ij} \begin{pmatrix} m & n \\ 0 & l \end{pmatrix}$, we infer that:

$$\Phi_{ij} \begin{pmatrix} m & n \\ 0 & l \end{pmatrix} = -\kappa_m e_i(m) e_j(m). \tag{25}$$

We consider below the example of the diatomic chain in order to illustrate the existence of acoustic and optic modes.

A. Acoustic and Optic modes

Let us consider a 1D diatomic chain made of a sequence of M_1 and $M_2 > M_1$ masses in the unit cell separated by a distance a and κ the elastic constant coupling them. Consequently the lattice constant is $2a$.

We omit the (ij) index from Φ_{ij} since we have a linear chain, we derive from the elastic energy involving relative displacements of M_1, M_2 in cell n and those of M_1 in cell $n+1$ and M_2 in cell n assuming that the same elastic constant κ is involved in all cases:

$$\sum_n \frac{\kappa}{2}[u(1,n) - u(2,n)]^2 + \frac{\kappa}{2}[u(1,n+1) - u(2,n)]^2 \tag{26}$$

Thus, the following force constant matrices are determined by picking the value $n = -1$ leading to cells numbered -1 and 0:

$$\Phi\begin{pmatrix}1,\ 2\\ 0,\ 0\end{pmatrix} = \Phi\begin{pmatrix}1,\ 2\\ 0,-1\end{pmatrix} = -\kappa\mathbb{1} \tag{27}$$

$\mathbb{1}$ is the unit 2×2 matrix and $\Phi\begin{pmatrix}1,\ 2\\ 0,\ 0\end{pmatrix}$ is a force constant matrix linking first and second atoms in cell 0 whereas $\Phi\begin{pmatrix}1,\ 2\\ 0,-1\end{pmatrix}$ relates first and second atoms in cell 0 and -1 respectively.

Matrix $\Phi\begin{pmatrix}1,\ 1\\ 0,\ 0\end{pmatrix}$ is found from the sum rule in equation (21) as:

$$\Phi\begin{pmatrix}1,\ 1\\ 0,\ 0\end{pmatrix} + \Phi\begin{pmatrix}1\ \ 2\\ 0,\ 0\end{pmatrix} + \Phi\begin{pmatrix}1,\ 2\\ 0,-1\end{pmatrix} = 0, \tag{28}$$

yielding $\Phi\begin{pmatrix}1,\ 1\\ 0,\ 0\end{pmatrix} = 2\kappa\mathbb{1}$

We derive from eq. 25 the matrices describing the forces involving the second atom in unit cell 0 as:

$$\Phi\begin{pmatrix}2,\ 1\\ 0,\ 1\end{pmatrix} = \Phi\begin{pmatrix}2,\ 1\\ 0,\ 0\end{pmatrix} = -\kappa\mathbb{1}.$$

Hence from the sum rule:

$$\Phi\begin{pmatrix}2,\ 2\\ 0,\ 0\end{pmatrix} + \Phi\begin{pmatrix}2,\ 1\\ 0,\ 1\end{pmatrix} + \Phi\begin{pmatrix}2,\ 1\\ 0,\ 0\end{pmatrix} = 0, \tag{29}$$

to yield $\Phi\begin{pmatrix}2,\ 2\\ 0,\ 0\end{pmatrix} = 2\kappa\mathbb{1}$.

The dynamical matrix is obtained from eq. 16 as:

$$D = \begin{pmatrix} \frac{2\kappa}{M_1} & -\frac{\kappa}{\sqrt{M_1M_2}}\left(1+e^{ika}\right) \\ -\frac{\kappa}{\sqrt{M_1M_2}}\left(1+e^{-ika}\right) & \frac{2\kappa}{M_2} \end{pmatrix} \tag{30}$$

The lower eigen-frequencies are acoustic and given by:

$$\omega_A^2 = \kappa\left(\frac{1}{M_1}+\frac{1}{M_2}\right) - \kappa\sqrt{\left(\frac{1}{M_1}+\frac{1}{M_2}\right)^2 - \frac{4\sin^2(ka)}{M_1M_2}}. \tag{31}$$

The acoustic term is due to the fact in the long-wavelength limit ($k \to 0$) $\omega_A \to v_s k$ with sound velocity $v_s = 2a\sqrt{\frac{\kappa/2}{(M_1+M_2)}}$.

whereas the higher eigen-frequencies (optic) are given by:

$$\omega_O^2 = \kappa\left(\frac{1}{M_1}+\frac{1}{M_2}\right) + \kappa\sqrt{\left(\frac{1}{M_1}+\frac{1}{M_2}\right)^2 - \frac{4\sin^2(ka)}{M_1M_2}}. \tag{32}$$

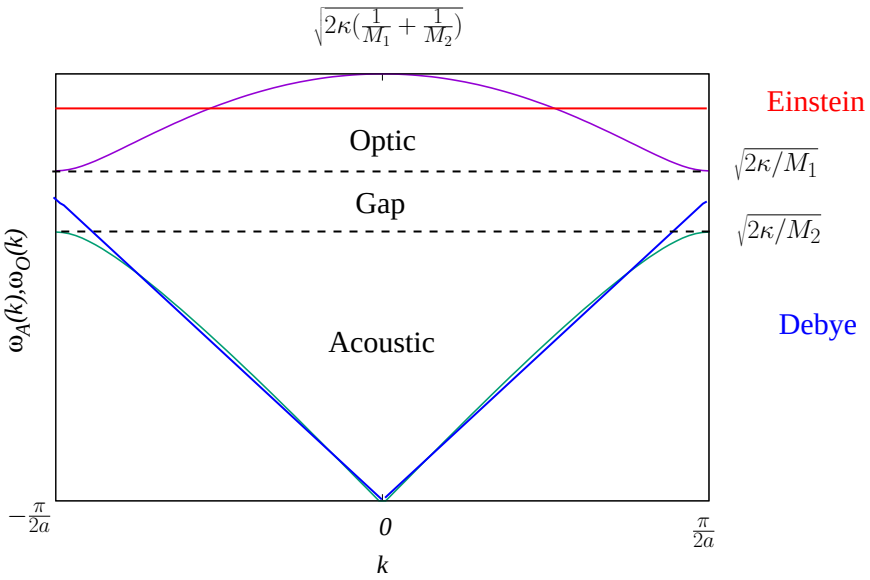


Fig. 4: (Color on-line) Acoustic $\omega_A(\boldsymbol{k})$ (green) and Optic $\omega_O(\boldsymbol{k})$ (magenta) phonon dispersion branches of the diatomic chain. Their symmetry stems from Kramers theorem proper to time reversal symmetry yielding $\omega_A(\boldsymbol{k}) = \omega_A(-\boldsymbol{k})$ and $\omega_O(\boldsymbol{k}) = \omega_O(-\boldsymbol{k})$ (see section IV B). Einstein (red) and Debye (blue) approximations are displayed. The exact acoustic dispersion is very close to the Debye approximation with a slope equal to the sound velocity $v_s = 2a\sqrt{\frac{\kappa/2}{(M_1+M_2)}}$. The energy gap between $\sqrt{\frac{2\kappa}{M_1}}$ and $\sqrt{\frac{2\kappa}{M_2}}$ values is visible between the acoustic (green) and optic (magenta) branches. Debye (blue) linear dispersion curve violates Bragg reflection forcing flat dispersion at the Brillouin zone boundaries and makes an incursion in the gap region.

In the long-wavelength limit ($k \to 0$) $\omega_O \to$ non-zero constant equal to $\sqrt{2\kappa\left(\frac{1}{M_1}+\frac{1}{M_2}\right)}$.

Since masses M_1, M_2 are different, there is a gap between the bands at the zone boundaries $\pm(\pi/2a)$ (see fig. 4).

In the case of more complicated systems, Group theory is very useful in determining the properties and symmetries of the force constant matrices as well as the form of the eigenvalue equations (see for example ref.[12]).

B. Vibrational density of states

The density of states $g(\omega)$ is defined such that the number of k states in the interval $[\omega, \omega + d\omega]$ is such that:

$$g(\omega)d\omega = \sum_{\substack{\lambda,\boldsymbol{k} \\ \omega \le \omega_\lambda(\boldsymbol{k}) \le \omega + d\omega}} \tag{33}$$

where $\omega_\lambda(\boldsymbol{k})$ is the dispersion relation of a phonon branch indexed with $\lambda \in [1, \nu d]$. d is system dimension and ν is the number of atoms/molecules per unit cell. There are d acoustic branches and $\nu(d-1)$ optic branches at higher energy. For instance, diamond is made of two FCC lattices displaced by $(\frac{1}{4}, \frac{1}{4}, \frac{1}{4})$ with respect to one another[5]. Thus diamond has two Carbon atoms in the unit cell and consequently $\nu = 2$ yielding six phonon branches in 3D: three acoustic and three optic[13].

The density of states (DOS) is generally determined from the group velocity and in 1D $g(\omega) = \frac{L}{\pi|v_g|}$ where the 1D group velocity is $v_g = \frac{d\omega}{dk}$ and L is the system typical linear length. Thus $g(\omega) = \frac{L}{\pi}|\frac{dk}{d\omega}|$.

In d dimensions, Kittel[5] defines the density of states $g(\omega)$ for a system of typical linear length L as given by $g(\omega) = \left(\frac{L}{2\pi}\right)^d \int \frac{dS_\omega}{v_g}$ with $\boldsymbol{k}$ integration performed such that $\omega < \omega(\boldsymbol{k}) < \omega + d\omega$. v_g is the d dimension group velocity modulus of the vibration excitations[5]: $v_g = |\nabla_{\boldsymbol{k}}\omega(\boldsymbol{k})|$ and dS_ω is the differential area element on the constant surface $\omega(\boldsymbol{k}) = \omega$.

Specializing to the Debye case $\omega_D(\boldsymbol{k}) = v_g|\boldsymbol{k}| = v_g k$, the above expression of the density of the states can be expressed analytically since the constant energy surface $\omega(\boldsymbol{k}) = \omega$ is a hypersphere with radius $k = \omega/v_g$ and surface equal to $S_\omega = s_d k^{d-1} = s_d(\omega/v_g)^{d-1}$ where s_d is the unity radius hypersphere surface given by[14] $s_d = 2\pi^{d/2}/\Gamma(d/2)$. For instance, $s_d = (2, 2\pi, 4\pi)$ for $d = (1, 2, 3)$.

The d dimension Debye density of states is: $g_D(\omega) = \left(\frac{L}{2\pi}\right)^d \frac{S_\omega}{v_g}$ that is $g_D(\omega) = \left(\frac{L}{2\pi}\right)^d \frac{1}{v_g}\frac{2\pi^{d/2}}{\Gamma(d/2)}\left(\frac{\omega}{v_g}\right)^{d-1}$. In 3D we get $g_D(\omega) = \frac{V_c\omega^2}{2\pi^2 v_g^3}$ as used in section III with v_g replacing v_λ and $V_c = L^3$ the 3D system volume.

Note that in the Debye case, there is a cutoff frequency obtained from the condition that the total number of modes per acoustic branch is given by $\int_0^{\omega_c} g_D(\omega)d\omega = Nd$ where N is the number of cells.

The Einstein case is much simpler since the dispersion is a constant given by $\omega = \omega_E$ (constant) and consequently $g_E(\omega) = Nd\delta(\omega - \omega_E)$.

Specializing to the diatomic chain case we evaluate v_g from eq. 31 and eq. 32. Both equations are rewritten as: $\omega^2 = A \pm \sqrt{A^2 - C\sin^2(ka)}$ where $A = \kappa\left(\frac{1}{M_1} + \frac{1}{M_2}\right)$ and $C = \frac{4\kappa^2}{M_1 M_2}$. Performing the derivatives we get:

- Acoustic branch: $\left|\frac{dk}{d\omega}\right| = \frac{2\omega(A-\omega^2)}{a\sqrt{A^2-(\omega^2-A)^2}\sqrt{C-A^2+(\omega^2-A)^2}}$ for $0 \le \omega \le \sqrt{\frac{2\kappa}{M_2}}$.
- Optic branch: $\left|\frac{dk}{d\omega}\right| = \frac{2\omega(\omega^2-A)}{a\sqrt{A^2-(\omega^2-A)^2}\sqrt{C-A^2+(\omega^2-A)^2}}$ for $\sqrt{\frac{2\kappa}{M_1}} \le \omega \le \sqrt{2\kappa\left(\frac{1}{M_1} + \frac{1}{M_2}\right)}$

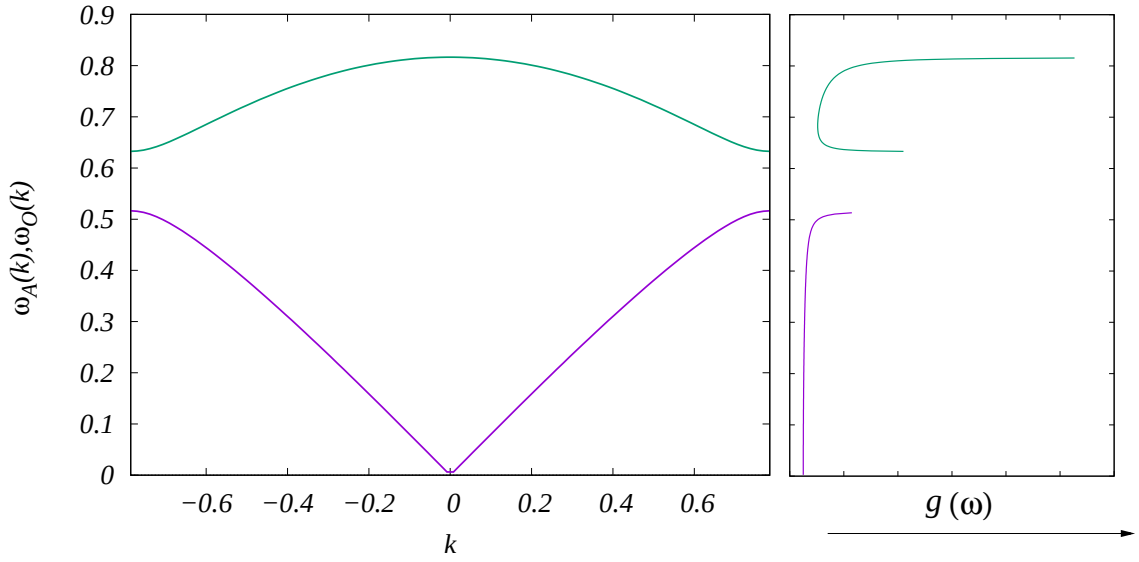


Fig. 5: (Color on-line) Phonon branches with k in $\pi/2a$ units and corresponding DOS. The acoustic DOS is almost constant since it is close to a Debye line (see fig.4) of the form $v_s k$ where v_s is sound velocity given by $2a\sqrt{\frac{\kappa/2}{(M_1+M_2)}}$. Given that, in the Debye approximation, the DOS $g(\omega) \sim \omega^{d-1}$ and $d = 1$ we get a constant $g(\omega) \sim \frac{L}{\pi|v_s|}$. Note the divergence of the acoustic DOS near the boundary zone at $\omega = \sqrt{\frac{2\kappa}{M_2}}$. The optic DOS show divergences near the boundary zone at $\omega = \sqrt{\frac{2\kappa}{M_1}}$ and near zone center ($k = 0$).

The DOS results in fig. 5 display a divergence in the acoustic branch due to the flattening (giving a zero v_g) of the dispersion close to the zone boundary as well as in the optic branch which has a divergence near the zone center due to flattening of the branch. Kramers theorem[5] implying time-reversal symmetry at Γ point ($k = 0$) induces flattening of the branches around zone center since $\omega(k) = \omega(-k)$ and an optic mode goes to a non-zero constant at long-wavelength limit.

To summarize, when ν the number of atoms/molecules per unit cell is larger than unity, we have two types of modes:

- Lower energy acoustic modes that correspond to in-phase vibrations behaving as $v_\lambda k$ when $k \to 0$ and flattening at zone borders due to Bragg reflections. In d dimensions, there are d acoustic branches.
- Higher energy optic modes that correspond to out-of-phase vibrations, flattening when $k \to 0$ to non-zero constant and additionally at zone borders due to Bragg reflections. In d dimensions, there are $\nu(d-1)$ optic branches.

V. APPLICATION TO GRAPHENE

Graphene has two Carbon atoms in the unit cell (see fig. 6), thus $\nu = 2$ and accordingly should have in 2D, two acoustic and two optic phonon branches. However we will be considering graphene as a monolayer of graphite oscillating in 3D (Z i.e. out of plane modes), consequently it has three acoustic and three optic phonon modes.

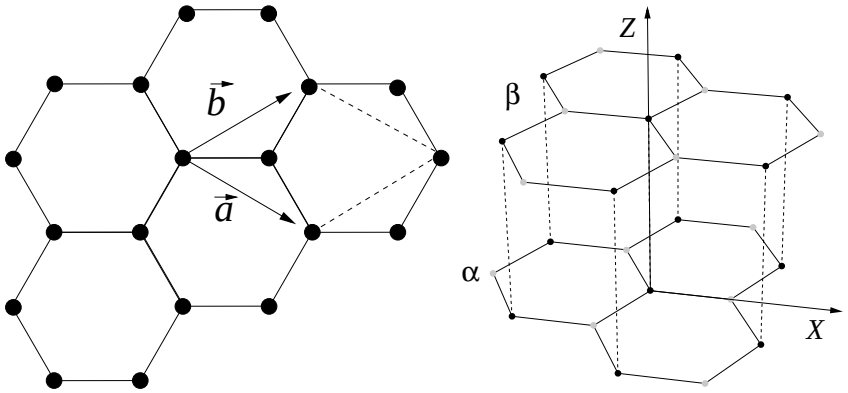


Fig. 6: Structure of 2D graphene (left) displaying a unit cell containing two Carbon atoms and 3D Graphite (right) with sublattices α and β.

There exist many approaches dedicated to the evaluation of graphene vibrations. One of the earliest approaches is by Woods and Mahan[15]. It is based on the existence of two energies:

- Central bond stretching (see Appendix A):

$$V_s = \frac{1}{2}\alpha_0 \sum_{i,j} \left[(\boldsymbol{u}_j - \boldsymbol{u}_i) \cdot \frac{\boldsymbol{r_{ij}}}{|\boldsymbol{r_{ij}}|} \right]^2 \tag{34}$$

- Bond bending based on three-body[16] interactions (see Appendix A):

$$V_b = \frac{1}{2}\beta_0 \sum_{i,j,k} (\cos\theta_{i,j,k} - \cos\theta_0)^2 \tag{35}$$

where $\theta_{i,j,k}$ is the angle between $i-j$ and $i-k$ bonds and θ_0 is the equilibrium angle of the crystal. It is, for instance, 120° in the case of graphite and graphene.

The angle $\theta_{i,j,k}$ is evaluated by:

$$\cos\theta_{i,j,k} = -\frac{1}{2} - \left(\frac{1}{2}\widehat{\boldsymbol{r_{ij}}} + \widehat{\boldsymbol{r_{ik}}}\right) \cdot (\boldsymbol{u}_i - \boldsymbol{u}_j) - \left(\frac{1}{2}\widehat{\boldsymbol{r_{ik}}} + \widehat{\boldsymbol{r_{ij}}}\right) \cdot (\boldsymbol{u}_i - \boldsymbol{u}_k) \tag{36}$$

Woods and Mahan[15] succeeded in capturing the essential features of graphene phonon dispersion displaying at the zone center (Γ point), two lower modes starting at zero frequency with higher modes starting from the same finite value. In addition, two modes, the longitudinal optic and acoustic, at the K point, are degenerate.

Woods and Mahan[15] derived the graphene phonon dispersion curves with only two constants namely α_0 = 58.98 N/m^2, β_0 = 50.4 N/m^2.

Another approach was made by Oshima *et al.*[17] who divided the vibration energy into five terms: nearest neighbor stretching, next nearest neighbor stretching, in-plane bending, out of plane bending (yielding Z acoustic and optic modes, see fig. 2) and finally twisting (see fig. 7).

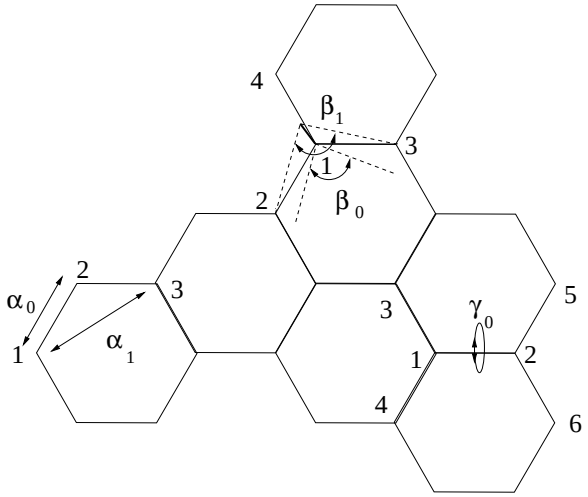


Fig. 7: (Color on-line) Vibration energy terms in graphene nearest neighbor stretching (α_0), next nearest neighbor stretching (α_1), in-plane bending (β_0), out of plane bending (β_1) and finally twisting (γ_0). Note the site numbering involved in every energy term.

The different energies (see fig. 7) are written as:

1. Nearest neighbor stretching:

$$\frac{1}{2}\alpha_0\left[(\boldsymbol{u}_2-\boldsymbol{u}_1)\cdot\frac{\boldsymbol{r_{12}}}{|\boldsymbol{r_{12}}|}\right]^2 \tag{37}$$

2. Next nearest neighbor stretching:

$$\frac{1}{2}\alpha_1\left[(\boldsymbol{u}_3-\boldsymbol{u}_1)\cdot\frac{\boldsymbol{r_{12}}}{|\boldsymbol{r_{13}}|}\right]^2 \tag{38}$$

3. In-plane bending:

$$\frac{\beta_0}{2}\left\{\left[(\boldsymbol{u}_2-\boldsymbol{u}_1)\times\frac{\boldsymbol{r_{12}}}{|\boldsymbol{r_{12}}|^2}\right]_z-\left[(\boldsymbol{u}_3-\boldsymbol{u}_1)\times\frac{\boldsymbol{r_{13}}}{|\boldsymbol{r_{13}}|^2}\right]_z\right\}^2 \tag{39}$$

Notation $|_z$ means out-of-plane component z of the mathematical quantity.

4. Out of plane bending:

$$\frac{\beta_1}{2}\left\{\frac{u_{2z}+u_{3z}+u_{4z}-3u_{1z}}{|\boldsymbol{r}|}\right\}^2 \tag{40}$$

where $|\boldsymbol{r}| = a_0\sqrt{3}$ with a_0 the hexagon side length.

5. Twisting:

$$\frac{\gamma_0}{2}\left[\frac{(u_{5z}-u_{6z})-(u_{3z}-u_{4z})}{a}\right]^2 \tag{41}$$

Tewary *et al.*[18] employed a more sophisticated approach using Tersoff-Brenner method to rederive the phonon dispersion curves and compare their results to experimental measurements[19,20]. They considered up to fourth neighbor interactions and their results when compared with experimental results fared quite well.

More precisely, the Tersoff-Brenner[21] potential they considered has 14 parameters that are obtained from experimentally measured cohesive energy, lattice constant, elastic constants C_{11} and C_{66}, flexural rigidity (or bending stiffness) YI (Y is Young modulus and I is moment of inertia) and phonon frequencies in three symmetry directions $\Gamma-K$, $\Gamma-M$ and $K-M$. Agreement between theory and experiment is shown in fig .8.

Regarding elastic constants C_{11} and C_{66}, the values obtained with the TB potential are respectively 846 GPa and 248 GPa. The values obtained by Tewary *et al.*[18] are C_{11}= 1060 GPa and C_{66}= 440 GPa, which are the measured values for graphite. Tewary *et al.*evaluated the mass normalized [1] flexural rigidity to be 2.13 eV whereas it is 0.797 eV when calculated using a second-neighbor TB model[21]. This means actually that the third and fourth neighbors make a substantial contribution to the flexural rigidity.

The 14 parameters intervene as elements into five generic force constant matrices that once are Fourier transformed yield the dynamical matrix whose eigenvalues yield the vibration eigenmodes. The force constant matrices are 3×3 since they account for the local three neighbor configuration typical of the hexagonal structure of graphene.

The success of this method is due to the fact the Tersoff-Brenner[21] potential is considered as one of the most accurate and faithful representation of Carbon-Carbon (Single, Double and Triple bonds) interactions in the case of both Diamond and Graphite. Moreover the TB potential showed it was able of describing faithfully sp^3 hybridized (like Diamond) and sp^2 hybridized systems[22] (like Graphite and Graphene).

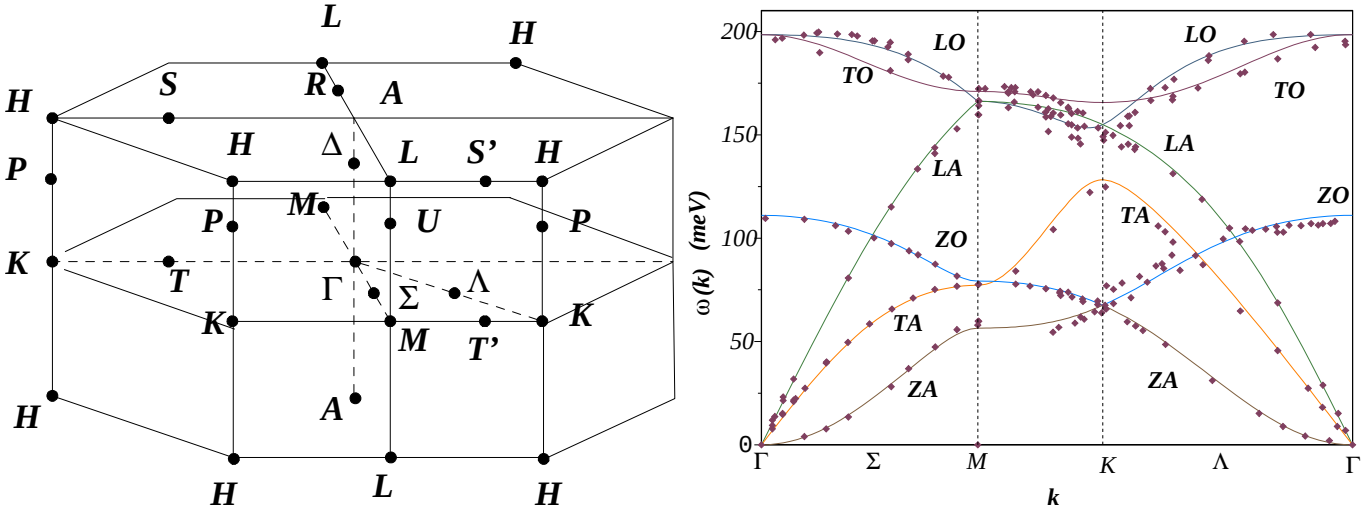


Fig. 8: (Color on-line) Brillouin zones (at left) of Graphite and Graphene, namely the hexagon at middle height which lies in the plane containing high-symmetry points Γ,K and M with relative distances $\Gamma-K=4\pi/3a$, $\Gamma-M=2\pi/\sqrt{3}a$, and $K-M=2\pi/3a$. Lattice parameter $a=2.463$ Å. Graphene phonon dispersion (at right) with out-of-plane modes along Z axis ZA and ZO. The comparison of theoretical and experimental results[19,23,24] is adapted from Tewary *et al.*[18] paper based on a parametric interaction potential of the Tersoff-Brenner[21] type.

Michel *et al.*[20] went even further to a fifth-nearest-neighbor force-constant model using Born method (see Appendix A) to calculate the stretching and bending coefficients of graphite in order to obtain the elastic constants, bulk modulus and sound velocities as displayed in Table I:

[1] The mass normalized flexural rigidity unit is eV whereas the real unit of YI is (dyn/cm).g.cm^2= dyn.g.cm= erg.g or eV.g. Note that in 2D the unit of Young modulus is dyn/cm (see Table II)

Elastic parameters	C_{11}	C_{12}	C_{66}	C_{33}	C_{44}	C_{13}	B	v_l	v_t
Born	1211.3	275.5	468.0	36.79	4.18	0.59	35.1	22.99	14.29
Ultrasonics and Static tests	1060	180	440	36.5	4.0	15			
Inelastic X rays	1109	139	485	38.7	5.0	0	36.4		

TABLE I: Table adapted from Michel *et al.*[20] showing elastic constants of graphite in GPa units (1 GPa=10^{10} dyn/cm^2) and sound velocities in km/s. As a rule of thumb, a 3D elastic constant C_{ij} is roughly[25] (Binding Energy) / (Bonding Volume). Taking Binding Energy ~ 1eV and Bonding Volume ~ ℓ^3 with ℓ ~ 1 Å we get C_{ij} ~ 1 Gpa. Theoretical results are given by the fifth-nearest-neighbor Born model whereas the experimental measurements are given either by Ultrasonics and Static tests or Inelastic X rays[20]. B is the bulk modulus[20] whereas v_l and v_t are longitudinal and transverse sound velocities.

The adiabatic/isothermal bulk modulus is given by: $B_{S,T} = -V\left(\frac{\partial P}{\partial V}\right)_{S,T}$ and using the Jacobian method (see Appendix B) we have $B_S \sim B_T \equiv B$, that is $B = \frac{C_{33}(C_{11}+C_{12})-2C_{13}^2}{(C_{11}+C_{12})+2C_{33}-4C_{13}}$ whereas v_l and v_t are longitudinal and transverse sound velocities given by $v_l = \sqrt{\frac{C_{11}}{\rho}}$, $v_t = \sqrt{\frac{C_{66}}{\rho}}$ where ρ is the graphite density.

In the graphite case, the agreement between Born theory and experiment is good and paves the way towards the experimentally difficult graphene case for which we have some theoretical results collected in Table II.

Elastic parameters	C_{11}	C_{66}	v_l	v_t
Michel *et al.*[20]	40.5	15.66	23.08	14.34
First principles[26]	38.5 (a), 51.5 (b)	19.5 (c)	26.0	16.0
In-plane graphite[27]	37.37 (d)	16.35 (d)	22.16	14.66

TABLE II: Table adapted from Michel *et al.*[20] showing 2D elastic constants C_{11} and C_{66} of graphene in 10^4 dyn/cm units and longitudinal v_l (resp. transverse v_t) sound velocities in km/s. As a rule of thumb a 2D elastic constant C_{ij} is roughly[25] (Binding Energy)/(Bonding Surface). Taking Binding Energy ~ 1eV and Bonding Surface ~ ℓ^2 with ℓ ~ 1 Å we get C_{ij} ~ 10^4 dyn/cm. Additional notes: a: Elastic stiffness value is 63 eV/atom. b: Obtained from v_l = 26 km/s. c: Obtained from v_t = 16 km/s. d: Evaluated with v_l = 22.16 km/s and v_t = 14.66 km/s.

The 2D bulk modulus and Young modulus evaluated for graphene are respectively $B_{2D} = 24.89 \times 10^4$ dyn/cm and $Y_{2D} = 38.46 \times 10^4$ dyn/cm. On the experimental side, mechanical measurements of graphene elastic constants are not trivial because of the nature of the material, nevertheless some progress is being observed[28].

APPENDIX A: ARBITRARY 3D SPRING DEFORMATION ENERGIES

There are many approaches[13] to the description of crystal vibration energies. They range from classical to a hybrid semi-classical mixture between classical and finally to full quantum.

There exist varieties of stretching, bending, twisting, breathing, rocking... energies ranging from 1D to full 3D and the spatial interaction extent varies from nearest neighbors to remote ones at larger distances such as second, third order neighbors...

Vibrations depend generally on force constants that are measured experimentally from thermodynamic quantities such as specific heat and thermal conductivity. Mechanical measurements yield elastic constants, compressibility and flexural rigidity (bending stiffness or ability to resist bending) given by YI where Y is Young modulus and I the moment of inertia. Structural measurements with X-Ray diffraction help in the determination of cohesion energy, equilibrium lattice parameters and angles. Neutron scattering helps also in the determination of elastic constants[5] and is extremely valuable since it allows a direct comparison between actual phonon dispersion curves and predicted ones from modeling.

Some of the approaches[13] are based on introducing descriptions pertaining to ionic displacements only with their stretching, bending... (valence, shell models) or introducing polarization effects (dipole models)... Some crystals like molecular or Van Der Waals behave like individual molecules and require radial deformations, whereas covalent

semiconductors behave like large molecules implying the use of valence models with radial and angular deformations... Other crystals like metals require inclusion of interaction with electrons in the surrounding Fermi sea, magnetic crystals require a distinction between spin up and spin down electrons...

Microscopic models based on many-body approaches (Green functions and inverse dielectric function) and ab-initio treatments based on full quantum calculations like DFT (Density Functional Theory) have also been performed successfully[13].

1. Stretching deformation energy

Arbitrary deformation of a spring (cf Fig. 9) in 3D is dealt through writing the potential energy as:

$$V = \frac{1}{2}\kappa(\Delta\ell)^2 \tag{A1}$$

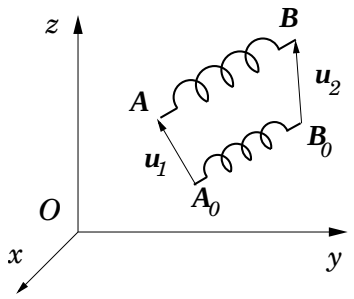


Fig. 9: Deformation of a spring with an arbitrary 3D spatial orientation.

where $\Delta\ell = |\boldsymbol{AB}| - |\boldsymbol{A_0B_0}| = |\boldsymbol{A_0B_0} + \boldsymbol{u}_2 - \boldsymbol{u}_1| - |\boldsymbol{A_0B_0}|$ and κ the spring constant.
Calling $\boldsymbol{u} = \boldsymbol{u}_2 - \boldsymbol{u}_1$ we get: $\Delta\ell = |\boldsymbol{A_0B_0} + \boldsymbol{u}| - |\boldsymbol{A_0B_0}|$.
This is rewritten as: $\Delta\ell = \sqrt{(\boldsymbol{A_0B_0} + \boldsymbol{u}) \cdot (\boldsymbol{A_0B_0} + \boldsymbol{u})} - |\boldsymbol{A_0B_0}|$.
Neglecting second order terms we get: $\Delta\ell \approx \sqrt{(\boldsymbol{A_0B_0})^2 + 2\boldsymbol{u} \cdot \boldsymbol{A_0B_0}} - |\boldsymbol{A_0B_0}|$.
Factoring $|\boldsymbol{A_0B_0}|$ we get: $\Delta\ell \approx |\boldsymbol{A_0B_0}|\sqrt{1 + 2\frac{\boldsymbol{u}\cdot\boldsymbol{A_0B_0}}{|\boldsymbol{A_0B_0}|^2}} - |\boldsymbol{A_0B_0}|$ that is: $\Delta\ell \approx \frac{\boldsymbol{u}\cdot\boldsymbol{A_0B_0}}{|\boldsymbol{A_0B_0}|}$.
This can be written compactly as: $\Delta\ell \approx \boldsymbol{u} \cdot \frac{\boldsymbol{r_{12}}}{|\boldsymbol{r_{12}}|} = \boldsymbol{u} \cdot \widehat{\boldsymbol{r_{12}}}$ where $\widehat{\boldsymbol{r_{12}}} = \frac{\boldsymbol{r_{12}}}{|\boldsymbol{r_{12}}|} = \frac{\boldsymbol{A_0B_0}}{|\boldsymbol{A_0B_0}|}$.
As a result, the potential energy takes the form:

$$V = \frac{1}{2}\kappa(\Delta\ell)^2 = \frac{1}{2}\kappa\left[(\boldsymbol{u}_2 - \boldsymbol{u}_1) \cdot \frac{\boldsymbol{r_{12}}}{|\boldsymbol{r_{12}}|}\right]^2 \tag{A2}$$

For a set of 3D springs, we generalize this formula as a pairwise ij sum:

$$V = \frac{1}{2}\sum_{i,j}\kappa_{ij}\left[(\boldsymbol{u}_j - \boldsymbol{u}_i) \cdot \frac{\boldsymbol{r_{ij}}}{|\boldsymbol{r_{ij}}|}\right]^2 \tag{A3}$$

In the case of a set of 1D aligned springs having different constants, the potential energy is written as:

$$V = \frac{1}{2}\sum_{i,j}\kappa_{ij}\left[(\boldsymbol{u}_j - \boldsymbol{u}_i)\right]^2 \tag{A4}$$

where κ_{ij} is the spring constant between sites i, j.

2. Bending deformation energy

In order to evaluate the bending energy, the angular distortion must be handled and then an expansion ought to be performed in the small distortion case as we did in the stretching case. Thus the simplest stretching and bending energy are given by the Born[13] model:

$$V = \frac{1}{2}\sum_{i,j}\alpha_{ij}\left[(\boldsymbol{u}_j - \boldsymbol{u}_i)\cdot\frac{\boldsymbol{r_{ij}}}{|\boldsymbol{r_{ij}}|}\right]^2 + \frac{1}{2}\sum_{i,j}\beta_{ij}(\boldsymbol{u}_j - \boldsymbol{u}_i)^2 \tag{A5}$$

where β_{ij} are bending constants akin to the stretching constants α_{ij}.
The Keating[13] model contains a more elaborate stretching and bending energies:

$$V = \frac{3}{4}\alpha_K\sum_{i,j}\left[(\boldsymbol{u}_j - \boldsymbol{u}_i)\cdot\frac{\boldsymbol{r_{ij}}}{|\boldsymbol{r_{ij}}|}\right]^2 + \frac{3}{16}\beta_K\sum_{i,(j,k)}\left[(\boldsymbol{u}_j - \boldsymbol{u}_i)\cdot\frac{\boldsymbol{r_{ik}}}{|\boldsymbol{r_{ik}}|} + (\boldsymbol{u}_i - \boldsymbol{u}_k)\cdot\frac{\boldsymbol{r_{ij}}}{|\boldsymbol{r_{ij}}|}\right]^2 \tag{A6}$$

where the indexed sum $i,(j,k)$ means it is performed over triplets of neighboring atoms and α_K, β_K are stretching and bending parameters.
In the case of graphene, another form of bending energy between a triplet (1,2,3) of neighboring atoms is given by:

$$\frac{\beta}{2}\left\{\left[(\boldsymbol{u}_2 - \boldsymbol{u}_1)\times\frac{\boldsymbol{r_{12}}}{|\boldsymbol{r_{12}}|^2}\right]_z - \left[(\boldsymbol{u}_3 - \boldsymbol{u}_1)\times\frac{\boldsymbol{r_{13}}}{|\boldsymbol{r_{13}}|^2}\right]_z\right\}^2 \tag{A7}$$

In fact, it originates from the equilibrium angular constraint of 120° .
Notation $|_z$ means out-of-plane component z of the mathematical quantity and β is the main bending parameter.
In the case of Silicon and similar semiconductors, the most representative bending energy is related to the distortion of the tetrahedron structure and the most popular approach was done by Stillinger and Weber[16] through the introduction of a combinatorial function of a three-body angle $\theta_{i,j,k}$ with a permuted index:

$$f_3(\boldsymbol{r_i}, \boldsymbol{r_j}, \boldsymbol{r_k}) = h(\boldsymbol{r_{ij}}, \boldsymbol{r_{ik}}, \theta_{j,i,k}) + h(\boldsymbol{r_{ji}}, \boldsymbol{r_{jk}}, \theta_{i,j,k}) + h(\boldsymbol{r_{ki}}, \boldsymbol{r_{kj}}, \theta_{i,k,j}) \tag{A8}$$

based on a three-body potential function limited by a cutoff length a:

$$h(\boldsymbol{r_{ij}}, \boldsymbol{r_{ik}}, \theta_{j,i,k}) = \lambda\exp[\gamma(r_{ij} - a)^{-1} + \gamma(r_{ik} - a)^{-1}]\left(\cos\theta_{j,i,k} + \frac{1}{3}\right)^2 \tag{A9}$$

λ, γ are parameters. The factor $(\cos\theta_{j,i,k} + \frac{1}{3})^2$ favors the perfect tetrahedral structure with angle θ_0 such that $\cos\theta_0 = -\frac{1}{3}$. Thus θ_0 value is given by $\cos^{-1}(-1/3) = 109.47°$ in the case of diamond and tetrahedral structure semiconductors like Si, Ge, GaAs...

Finally, note that the bending energy can be written in a more appealing way[15] as:

$$\frac{\beta}{2}\sum_{ijk}(\cos\theta_{ijk} - \cos\theta_0)^2 \tag{A10}$$

leading immediately to the hexagonal value $\theta_0 = 120°$ for graphite and graphene and the tetrahedral angle $\theta_0 = \cos^{-1}(-1/3) = 109.47°$ in the case of Diamond and diamond-like semiconductors such as Si, Ge, GaAs...

APPENDIX B: NOTE ON THE BULK MODULUS

If we want to find the expression of B_S, we start by writing: $B_S = -V\left(\frac{\partial P}{\partial V}\right)_S$ using two mathematical tools:

1. The Jacobians[29,30] with the following properties:

   - $\frac{\partial(u,v)}{\partial(x,y)} = \begin{vmatrix} \frac{\partial u}{\partial x} & \frac{\partial u}{\partial y} \\ \frac{\partial v}{\partial x} & \frac{\partial v}{\partial y} \end{vmatrix}$

- $\frac{\partial(u,v)}{\partial(x,y)} = -\frac{\partial(v,u)}{\partial(x,y)}$
- $\frac{\partial(u,y)}{\partial(x,y)} = \left(\frac{\partial u}{\partial x}\right)_y$
- $\frac{\partial(u,v)}{\partial(x,y)} = \frac{\partial(u,v)}{\partial(s,t)}\frac{\partial(s,t)}{\partial(x,y)}$
- $\frac{\partial(u,v)}{\partial(x,y)} = 1/\frac{\partial(x,y)}{\partial(u,v)}$

2. Maxwell identities which are given by the mnemonic matrix $\begin{vmatrix} PS \\ TV \end{vmatrix}$ yielding: $\left(\frac{\partial P}{\partial T}\right)_V = \left(\frac{\partial S}{\partial V}\right)_T$ and each time we exchange variables diagonally we pick up a sign change as in the case $P \leftrightarrow V$: $\begin{vmatrix} VS \\ TP \end{vmatrix}$ equivalent to: $\left(\frac{\partial V}{\partial T}\right)_P = -\left(\frac{\partial S}{\partial P}\right)_T$.

Any term such as $\partial(x,y)$ behaves as if it were an algebraic coefficient simplifying enormously the mathematical manipulations.

However there is a limit to express any physical quantity: It should depend on three measurable quantities[29]:

1. Dilation coefficient $\alpha_P = \frac{1}{V}\left(\frac{\partial V}{\partial T}\right)_P$
2. Compressibility $\kappa_T = -\frac{1}{V}\left(\frac{\partial V}{\partial P}\right)_T$
3. Heat capacity $C_V = T\left(\frac{\partial S}{\partial T}\right)_V$ or $C_P = T\left(\frac{\partial S}{\partial T}\right)_P$

If we want to find the expression of B_S. We start by writing: $B_S = -V\left(\frac{\partial P}{\partial V}\right)_S$ which gives:

$B_S = -V\frac{\partial(P,S)}{\partial(V,S)} = -V\frac{\partial(P,S)}{\partial(V,T)}\frac{\partial(V,T)}{\partial(V,S)} = -V\begin{vmatrix} \left(\frac{\partial P}{\partial V}\right)_T & \left(\frac{\partial P}{\partial T}\right)_V \\ \left(\frac{\partial S}{\partial V}\right)_T & \left(\frac{\partial S}{\partial T}\right)_V \end{vmatrix}\left(\frac{\partial T}{\partial S}\right)_V$.

This is transformed into: $B_S = -V\begin{vmatrix} -\frac{1}{V\kappa_T}\left(\frac{\partial P}{\partial T}\right)_V & \frac{T}{C_V} \\ \left(\frac{\partial S}{\partial V}\right)_T & \frac{C_V}{T} \end{vmatrix}$.

Developing the determinant we get: $B_S = -\frac{VT}{C_V}\left(-\frac{C_V}{VT\kappa_T} - \left(\frac{\partial P}{\partial T}\right)_V\left(\frac{\partial S}{\partial V}\right)_T\right)$

Maxwell relations yield: $\left(\frac{\partial S}{\partial V}\right)_T = \left(\frac{\partial P}{\partial T}\right)_V$ and the Jacobian method gives: $\left(\frac{\partial P}{\partial T}\right)_V = -\left(\frac{\partial V}{\partial T}\right)_P\left(\frac{\partial P}{\partial V}\right)_T = \alpha_P V\frac{1}{VT\kappa_T} = \frac{\alpha_P}{\kappa_T}$.

Thus $B_S = \frac{VT}{C_V}\left(\frac{C_V}{VT\kappa_T} + \left(\frac{\partial P}{\partial T}\right)_V^2\right)$. and finally $B_S = B_T + \frac{VT}{C_V}\alpha_P^2 B_T^2$.

Since for a solid the dilation coefficient is relatively small, consequently: $B_S \sim B_T$.

---

[1] E. Bright Wilson Jr., J.C. Decius and P. C. Cross, *Molecular Vibrations*, McGraw-Hill, New-York (1955).
[2] A. Nussbaum, Am. J. Phys., **36**, 529 (1968).
[3] G. Venkataraman and V.C. Sahni, Rev. Mod. Phys. **42**, 409 (1970). See also G. Venkataraman, L. A. Feldkamp, and V.C. Sahni, *Dynamics of perfect crystals*, MIT Press, Cambridge (1975).
[4] W. DeSorbo, J. Chem. Phys. **11**, 876 (1953).
[5] C. Kittel, *Introduction to Solid State Physics*, 8th edition, Wiley, New-York (2005).
[6] F. B. Hildebrand, *Advanced Calculus for Applications*, p. 359, Prentice-Hall, London (1962).
[7] P. Debye, Annalen der Physik, **38**, 789 (1912).
[8] O. Madelung, *Introduction to solid state theory*, Springer-Verlag (1996).
[9] M. Abramowitz and I.S Stegun, *Handbook of Mathematical Tables*, Dover, New-York (1960).
[10] E. Dubinov and A. A. Dubinova, *Exact Integral-Free Expressions for the Integral Debye Functions*, Technical Physics Letters, Vol. 34, 999 (2008).
[11] U. Rössler, *Solid State Theory: An introduction*, Second Edition, Springer-Verlag (2009).
[12] M. El-Batanouny and F. Wooten *Symmetry and Condensed Matter Physics: A Computational approach*, Cambridge University Press (2008).
[13] H. Bilz, and W. Kress, *Phonon Dispersion Relations in Insulators*, Springer-Verlag, Berlin (1979).
[14] F. Reif, *Statistical and Thermal Physics*, McGraw-Hill, New-York (1985).
[15] L. M. Woods and G. D. Mahan Phys. Rev. B **61**, 10651 (2000).
[16] F.H. Stillinger and T. A. Weber, Phys. Rev. B **31**, 5262 (1985).
[17] T. Aizawa, R. Souda, S. Otani, Y. Ishizawa and C. Oshima, Phys. Rev. B **42**, 11469 (1990).

[18] V. K. Tewary and B. Yang, Phys. Rev. B **79**, 075442 (2009).
[19] M. Mohr, J. Maultzsch, E. Dobardžić, I. Milošević, M. Damnjanović, A. Bosak, M. Krish, and C. Thomsen, Phys. Rev. B **76**, 035439 (2007).
[20] K. H. Michel and B. Verberck, Phys. Rev. B **78**, 085424 (2008).
[21] J. Tersoff, Phys. Rev. Lett. 61, 2879 (1988), W. Brenner, Phys. Rev. B 42, 9458 (1990)
[22] D. A. McQuarrie *Statistical Mechanics*, Harper and Row, New York (1973).
[23] L. Wirtz and A. Rubio, Solid State Commun. **131**, 141 (2004).
[24] S. Siebentritt, R. Pues, K. H. Rieder, and A. M. Shikin, Phys. Rev. B **55**, 7927 (1997).
[25] P. M. Chaikin and T. C. Lubensky, *Principles of Condensed Matter Physics* Cambridge University Press, Cambridge, England, (1995).
[26] O. Dubay and G. Kresse, Phys. Rev. B **67**, 035401 (2003).
[27] A. Bosak, M. Krisch, M. Mohr, J. Maultzsch, and C. Thomsen, Phys. Rev. **75**, 153408 (2007).
[28] Y. W. Sun, W. Liu, I. Hernandez, J. Gonzalez, F. Rodriguez, D. J. Dunstan, and C. J. Humphreys, *3D Strain in 2D Materials: To What Extent is Monolayer Graphene Graphite?* , Phys. Rev. Lett. **123**, 135501 (2019).
[29] H.B. Callen, *Thermodynamics and an introduction to thermostatistics*, 2nd edition, Wiley, New-York (1985).
[30] L. D. Landau and E. M. Lifshitz, *Statistical Physics, Part1*, Third Edition, Vol. 5, Pergamon, Oxford (1976).